

A TEST RIG FOR INVESTIGATIONS OF GAS TURBINE COMBUSTOR COOLING CONCEPTS UNDER REALISTIC OPERATING CONDITIONS

Thomas Behrendt, Christoph Hassa

DLR, German Aerospace Center

Institute of Propulsion Technology

Linder Höhe

D-51147 Cologne, Germany

Phone: +49/2203/601 – 2008

Fax: +49/2203/64395

E-Mail: thomas.behrendt@dlr.de

Keywords: *gas turbine combustor cooling, test facility*

Abstract

In this paper a new test rig for the characterization of advanced combustor cooling concepts for gas turbine combustors is introduced. The test rig is designed to allow investigations at realistic operating conditions of future lean combustors at elevated pressures and temperatures. The features and capabilities of the test rig in comparison to existing rigs are described. The properties of the hot gas flow are measured in order to provide the necessary data for an detailed analysis of the measured cooling efficiency of combustor wall test samples. Results of the characterization of the velocity and temperature distribution in the hot gas flow at the leading edge of the test sample at pressures up to $p = 10$ bar and global flame temperatures up to $T_F = 2000$ K are presented.

1 Introduction

Increasing air traffic, economic interests of the airlines and environmental issues lead to a general demand of more powerful and fuel efficient engines. These demands can be fulfilled by increasing the thrust efficiency (e. g. increased bypass ratio of the fan) and by rising the thermal efficiency of the core engine. The latter is

achieved with higher overall pressure ratios and with higher temperature levels at the turbine entry. Both measures have a disadvantageous effect on the production of nitric oxides (NO_x). Most of the NO_x emissions of aero engines are formed via the Zeldovich mechanism, see [1]. The NO_x production rate depends exponentially on the temperature. The combustor pressure, especially for conventional combustors, has an effect on the NO_x production rate mainly due to the effects of the homogenization of the fuel air mixture. Hence with present combustor technology future engines would not be able to meet the continuously tightening NO_x emission limits for the certification of new engines.

The most promising approach to reduce the NO_x emissions is to burn the fuel in a lean and more homogeneous mixture thus avoiding the high temperatures of near stoichiometric conditions, see [2]. Lean combustion concepts however require a completely different air flow distribution in the combustor. In order to achieve a fuel lean mixture with reference to the burner mass flow the fraction of the cooling air has to be reduced from up to 50 % of the combustor air in conventional combustors to less than 30 % in lean combustors, see [3, 4]. Novel combustor cooling

concepts have to be developed which allow this reduction of cooling air. Even with today's advanced CFD capabilities experimental investigations play a vital role in the understanding and development of combustor cooling technology.

2 Combustor Cooling Test Rigs

The different approaches to characterizing combustor cooling concepts experimentally can be divided basically into three groups. Most often isothermal low pressure test rigs are used, e. g. [5, 6, 7, 8]. These test rigs usually have a small temperature difference between the non-reacting main flow and the cooling air. They are especially well suited for characterising the interaction between the cooling film and the main flow and more fundamental heat transfer investigations. An approach to simulate a flow typical for gas turbine combustors is described in [9] where dilution jets and the cross sectional area reduction at the combustor exit are included in an isothermal test rig. The effect of the free stream turbulence on the cooling efficiency is analyzed by several investigations, e. g. [10, 11, 12]. These rigs offer an excellent accessibility for measuring equipment and well defined flow conditions. Most of the governing similarity parameters (e. g. Reynolds, Nusselt, Biot, blowing ratio) are kept constant in comparison to real combustor operating conditions. But other real combustor characteristics like velocity and temperature fluctuations can only be reproduced in test rigs with reacting flows.

The second group consists of test rigs where the exhaust gas of an combustor located upstream is utilized as the heat load on the test samples, e. g. [13, 14, 15]. These test rigs offer realistic temperature and velocity distributions and turbulence intensities at either atmospheric or elevated pressures. The spatial separation between hot gas generator and test cell creates a generic and typical heat load which is decoupled from the non-uniform heat release distribution in the burner near-field. By this means correlations of the total cooling effectiveness can be derived or validated under realistic operation conditions. Furthermore

the complexity of CFD calculations is limited to aspects of mixing and heat transfer allowing a more focused comparison between measured and computational results. On the other hand the accessibility for measuring techniques is reduced and the operating costs are higher. The new high pressure combustor cooling rig presented in this paper is classified into this second group of test rigs. The main features and differences to other test rigs will be described in section 3.

The test rigs in the third group use the combustor itself as a test section, see e. g. [16, 17], or multi sector combustors, e. g. [18, 4]. The heat load on the test sample is governed by the heat release distribution in the flame leading to a temperature and velocity distribution with inhomogeneities typical for combustors making this type of test rig more suitable for proof tests of cooling concepts. The access for measuring equipment is limited and obstructed by the flame and sometimes only permitting thermal paint tests.

3 DLR High Pressure Combustor Cooling Rig

The goal of the test rig is to offer a testing environment for metallic and ceramic test samples with operating conditions which are realistic for modern and future gas turbine combustors. The experimental results are also used to validate correlations of the cooling efficiency derived from data gathered at isothermal low pressure test rigs and for comparison with numerical CFD results. A scheme of the test rig is given in Fig. 1.

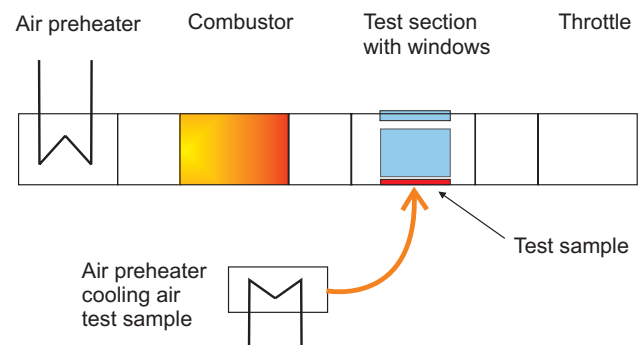


Fig. 1 Scheme of high pressure cooling test rig

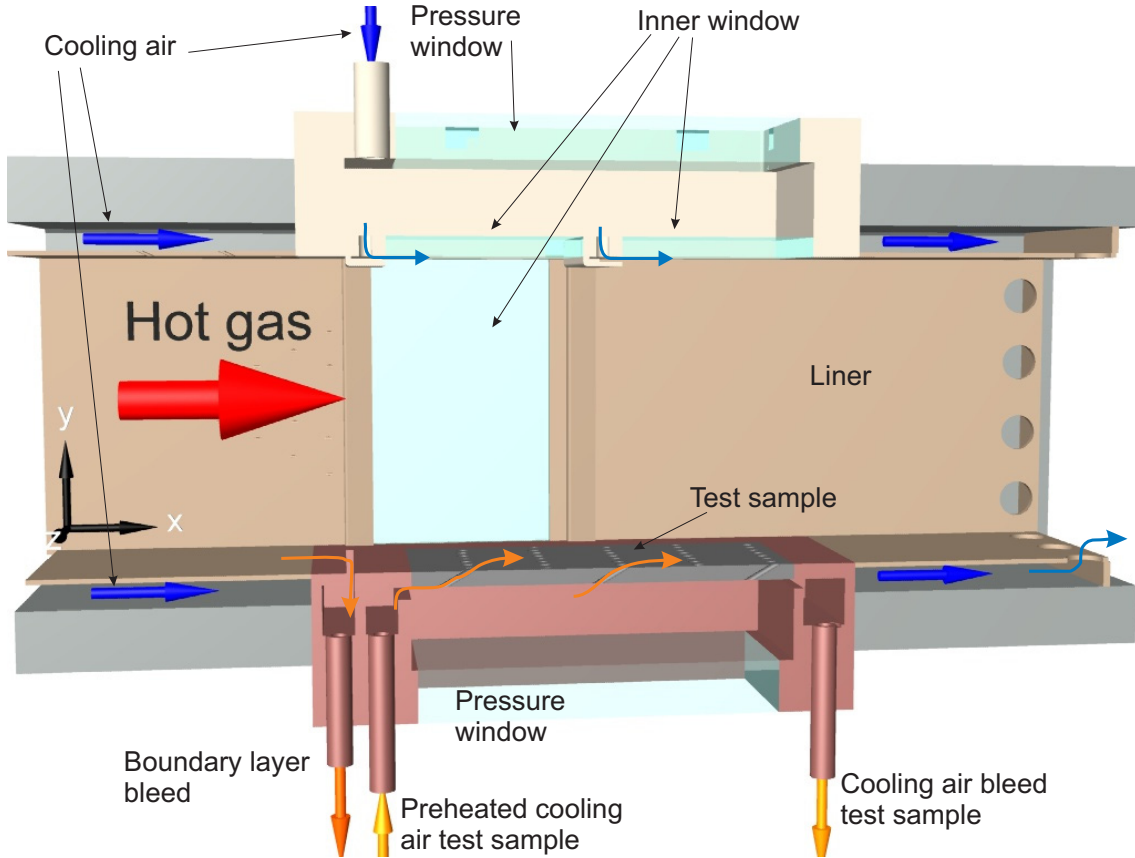


Fig. 2 Side view of the test section

A tubular water-cooled combustor is operated as a hot gas generator at pressures up to $p = 20$ bar. The preheated air flowing into the combustor is split into $\approx 70\%$ burner air and $\approx 30\%$ combustor head heat shield cooling air. Kerosene is burnt to produce an exhaust gas typical for future lean combustors. The global flame temperature T_F is the calculated equilibrium temperature based on the combustor air preheat temperature T_3 and the combustor equivalence ratio ϕ . The flame temperature can be set from $T_F = 1600 \dots 2100$ K. The bulk velocity u is calculated from the combustor mass flow, flame temperature, pressure and cross sectional area. The bulk velocity of the hot gas flow can be set between $u = 20 \dots 32$ m/s. For higher gas velocities a larger burner has to be installed in the combustor.

The hot gas is flowing through a water-cooled transition piece into the test section with a rect-

angular cross section where the combustor wall test sample is installed downstream of the combustor. The cross section of the test section is $A_{duct} = 80 * 103 \text{ mm}^2$. The combustor wall sample is $l = 100$ mm long (in main flow direction) and $b = 80$ mm wide. The pressure inside the combustor and the test section is built up by a water-cooled throttle. The cooling air of the test sample is preheated up to $T_{3,sample} \leq 750$ K by a separate air preheater. For non-intrusive optical measurement techniques the test section offers optical access to the test sample from all four sides, see Fig. 1 and 2.

The hot gas generated by the combustor is flowing through the liner, see Fig. 2. The liner is convectively cooled on the backside by cold air and has additional cooling fins. Furthermore at certain hot spots effusion cooling is applied. The cooling holes have a diameter of $d_{effu} = 0.6$ mm and are inclined with an angle of $\alpha_{effu} = 25^\circ$ rel-

ative to the liner surface. Special care was taken while defining the effusion cooled areas so that the swirl of the hot gas flow is not transporting additional cooling air to the test sample.

The handling of the thermal loads on the components upstream the test sample was an important aspect in the design of the test rig. As infrared thermography will be used to measure the temperature distribution on the test samples, the environment has to be as cold as possible. Hence every component (combustor, transition piece and liner) upstream of the test section is cooled and the convective heat losses create a temperature boundary layer. This boundary layer is blown out of the test section through a water cooled boundary layer bleed¹, see Fig. 2. The boundary layer bleed also removes the velocity boundary layer and is located at $x = -15$ mm upstream of the leading edge of the test sample.

The optical access to the hot gas side of the sample is realized by a double wall concept from three directions (two sidewalls and opposite wall). The inner windows are film cooled with cold air and take the heat load, see Fig. 2. The outer windows take the pressure load. The inner sidewall windows can be mounted in two different positions depending on the area where the optical access is needed (upstream or downstream part of the test sample).

The test sample is installed in a cassette to allow easy exchange of the samples. The preheated test sample cooling air is isolated from the liner cooling air, see Fig. 2. The temperature of the preheated cooling air ($T_{3,sample} \leq 750$ K) is measured on the backside of the sample. By a separate bleed the test sample cooling air mass flow and the pressure drop across the sample wall element can be set independently. Furthermore convectively cooled wall samples for combustors in industrial gas turbines can be investigated. On the rear side of the test sample a window can be installed to allow optical temperature measurements on the cooling air side of the sample.

¹For simplicity the water cooling is not shown in the sketch.

The test rig is equipped with a three axis traversing unit where optical measurement techniques like laser doppler anemometer or infra red camera are mounted. By this means techniques with a point-like measuring volume can scan the flow field. The resolution of the traversing unit is $\Delta = 0.1$ mm.

In a second stage a fuel rich burner as a radiation source will be taken into operation. This sooting burner will be installed instead of the window assembly opposite the test sample. By this means the cooling performance can be analysed under a convective and radiative heat load like in conventional combustors with a rich burning primary zone.

3.1 Comparison to other test rigs

In comparison to other test rigs in this group, see section 2, this test rig is designed for higher pressures and global flame temperatures. In contrast to the new facility in the test rigs described in [13, 14] the components upstream of the test section were uncooled and no boundary layer bleed was present.

Few information about the hot gas temperature and velocity distribution of the other test rigs is given in the open literature. In [13] a water-cooled perforated plate upstream the test sample is mentioned and a length scale for the grid is not reported. A velocity distribution comparable to the flow downstream of a mixing module of a conventional combustor can be assumed. The effect on the temperature distribution was not stated and the gas temperature was measured on the centerline of the flow.

In [14] spatial resolved temperature measurements were conducted. The combustor was set to produce hot gas at $T_F = 1000$ K. The low combustor temperature suggests that additional air was injected with the result that a very homogeneous temperature distribution was achieved. In [19, 20] velocity measurements at atmospheric pressure in the non-reacting and reacting flow respectively are reported for the same test rig revealing the same homogeneity as in the temperature distribution.

Operating point	Pressure p	Bulk temperature T_F	Bulk velocity u	Boundary layer bleed \dot{m}_{bleed}
TC1	5.0 bar	1750 K	24 m/s	8 g/s
TC2	5.0 bar	1750 K	30 m/s	8 g/s
TC3	5.0 bar	2000 K	30 m/s	12 g/s
TC4	10.0 bar	1750 K	30 m/s	15 g/s

Table 1 Operating conditions in test section

4 Operating conditions

The operating conditions of the hot gas generator and thus the bulk flow properties of the hot gas flow in the test section are defined by four quantities:

- Pressure p in the test section
- Calculated flame temperature T_F
- Bulk gas velocity u in main flow direction x
- Mass flow boundary layer bleed \dot{m}_{bleed}

The boundary layer bleed mass flow is mainly affecting the hot gas temperature distribution close to the wall. These quantities can be set independently over a wide range to allow investigations of the influence of a single flow property on the cooling efficiency of the test samples. The operating conditions where the hot gas flow was characterized are listed in Table 1. The combustor air was preheated to $T_3 = 650$ K.

5 Characterization of the hot gas flow

The characterization of the hot gas flow is essential for the analysis and interpretation of measured wall temperature distributions. Even though the combustor is located $l \approx 0.3$ m upstream of the test sample the velocity and temperature distributions are not fully homogenized. The heat shield cooling air in the combustor head and convective heat losses also contribute to this effect. Hence the bulk values are only suitable for identifying different operating conditions. Of particular interest are the flow properties at the leading edge of the sample. The measurements

are focused on the central part of the test sample ($y = -30 \dots 30$ mm) to avoid any interference with the cold window cooling air, see Fig. 3.

5.1 Gas velocity distribution

The actual hot gas velocity distribution is measured by Laser Doppler Anemometry (LDA). For a detailed description of the measuring principle see [21]. The laser beams and the scattered light are directed through the sidewall windows, see Fig. 3.

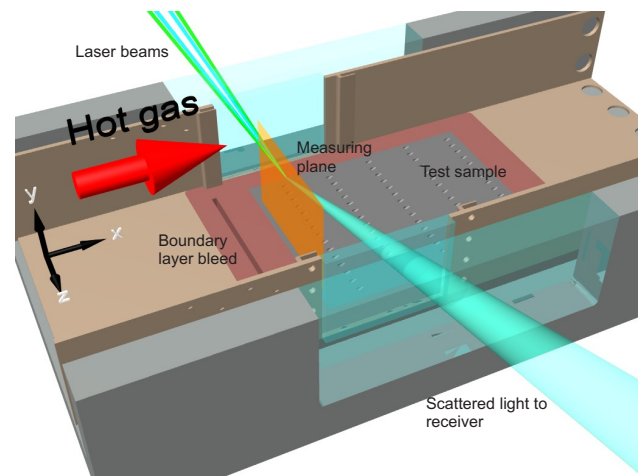


Fig. 3 Top view of the test section with LDA set up

With this set up the axial velocity u and the velocity v vertical to the test sample surface were measured. The measurement plane is located at $x = 2$ mm downstream of the leading edge of the test sample. This is about $\Delta x = 4$ mm upstream the first row of cooling holes. In order to enable velocity measurements close to the wall, it was necessary to tilt the transmitting optics by

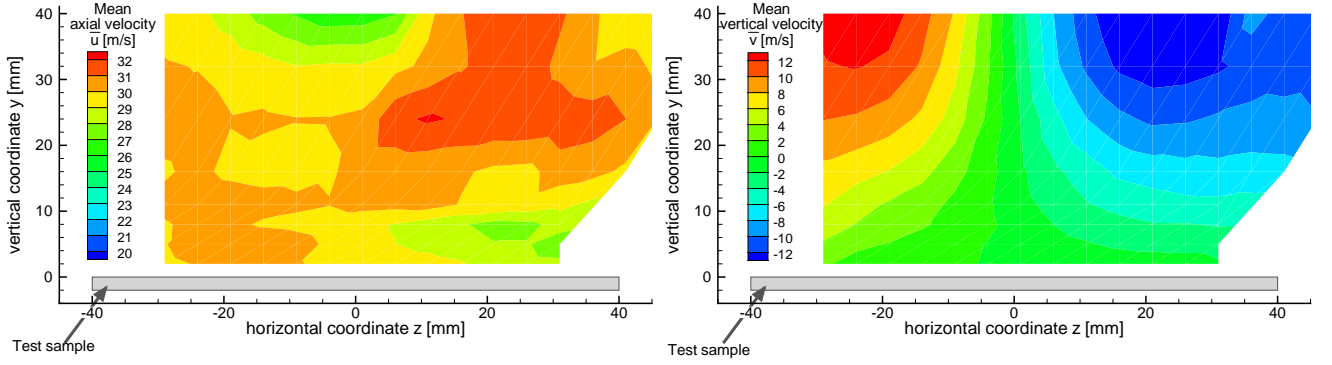


Fig. 4 Mean gas velocities \bar{u} and \bar{v} at TC2 ($p = 5$ bar, $T_F = 1750$ K and $u = 30$ m/s), view downstream

$\alpha \approx 2.2^\circ$. As the first vertical measurement position was $y = 2$ mm above the wall across the width of the test sample this rotation of the vertical component was accepted.

The combustor air was seeded with SiO_2 particles with a diameter of $d = 0.8 \mu\text{m}$. The scattered light was detected in forward direction to increase the signal to noise ratio. The electrical signals were processed by DANTEC Fast Fourier Transformation analyzers. At each measurement position 20000 particles were sampled or the acquisition was stopped after $\tau = 120$ sec. The Gaussian beam diameter of the measuring volume was $d_{mea} = 150 \mu\text{m}$ and the length of the measuring volume was $l_{mea} \approx 2$ mm.

In Fig. 4 the mean gas velocities for the operating point TC2 (see Table 1) are shown. The distribution of the mean axial velocity \bar{u} is fairly homogeneous. The lower velocities in the core of the flow ($y = 40$ mm and $z = 0$ mm) are caused by the central recirculation zone in the swirling burner flow field inside the combustor. The horizontal asymmetry is due to the fact, that at low pressures the burner was operated below its design operating range. At TC4 ($p = 10$ bar) the mean axial velocities show a much better symmetry, see Fig. 5.

The mean vertical velocities \bar{v} in Fig. 4 right is characteristic for a swirling burner flow field. Close to the wall ($y = 2$ mm) the flow is almost parallel to the wall. In the vertical plane of sym-

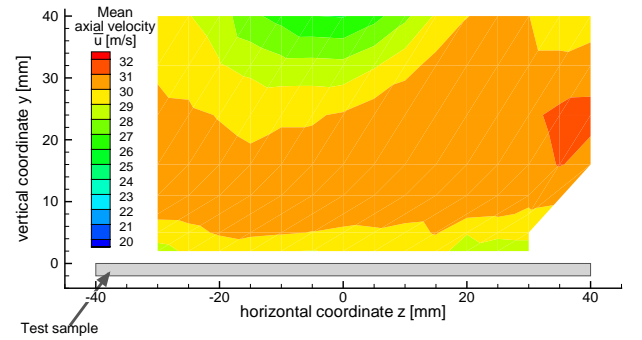


Fig. 5 Mean gas velocities \bar{u} at TC4 ($p = 10$ bar, $T_F = 1750$ K and $u = 30$ m/s), view downstream

metry ($y = 40$ mm) the vertical velocity corresponds to the tangential velocity.

A comparison of the mean axial velocities \bar{u} and vertical velocities \bar{v} close to the wall is given in Fig. 6 top and bottom respectively for all operating conditions. All profiles are even and show no significant inhomogeneities. The profiles of the axial velocities for the conditions with $u = 30$ m/s (solid lines) are almost independent of the pressure p and the flame temperature T_F . Comparing the profiles for $u = 30$ m/s with $u = 24$ m/s reveals no effect on the qualitative velocity distribution. The profiles of the vertical velocities \bar{v} in Fig. 6 bottom are virtually independent of the operating conditions. The asymmetry can be attributed to the swirl in the flow and is small in comparison to the order of magnitude of the axial velocities.

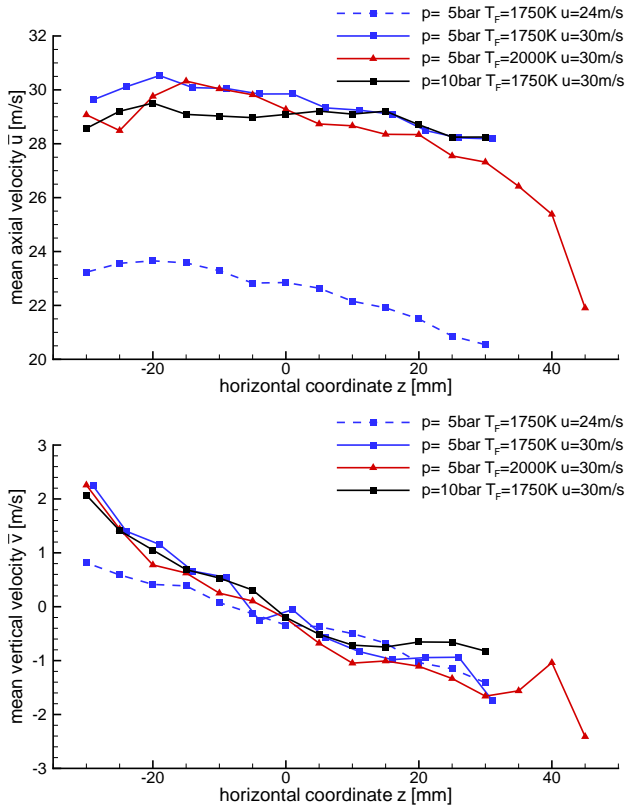


Fig. 6 Profiles of mean axial velocities \bar{u} (top) and vertical velocities \bar{v} (bottom) for different operating conditions at $y = 2$ mm

In Fig. 7 the turbulence levels of the axial velocity $Turb_u$ are shown. The turbulence levels show only a small influence of the operating conditions. The importance of including turbulence levels realistic for combustors into cooling investigations is emphasized by several authors of isothermal investigations, see e. g. [10, 11, 12]. The overall turbulence level of $Turb_u = 19 \dots 24\%$ in this test rig corresponds to the levels considered as relevant in the cited literature.

5.2 Gas temperature distribution

Beside the gas velocities also the gas temperature distribution near the wall had to be determined. Due to the measuring position it was not possible to apply optical temperature measurement techniques like CARS, see e. g. [22, 23]. Light sheet techniques as well were difficult to apply close to an opaque wall. Hence the tem-

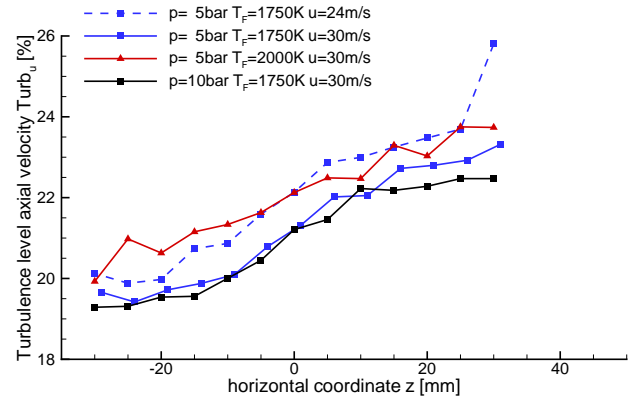


Fig. 7 Profiles of axial velocity turbulence levels $Turb_u$ for different operating conditions at $y = 2$ mm

perature distribution in the hot gas flow close to the wall was characterized by thermocouples. As introducing a traversable thermocouple probe into the pressure casing was not possible, a wall sample equipped with five type K thermocouples had to be used. The thermocouples were unsheathed and the junctions had a diameter of $d \approx 0.9$ mm. They were installed so that they measure the temperature at $x = -4$ mm upstream the leading edge of the sample $y = 3$ mm above the wall. To ensure fixed measuring positions of the thermocouples they were welded into the wall sample $\Delta x = 9.5$ mm downstream the measuring position. The thermocouples were located at $z = -30, -15, 0, 15, 30$ mm in lateral direction.

Measuring high gas temperatures with thermocouples is in principle a complex superposition of different heat transfer modes. A correction has to be applied to the measured temperatures to account for the convective heat transfer into the thermocouple and for radiative heat losses and conductive heat transfer between junction, wiring sheath and insulation of the thermocouple. The thermocouple was modelled by a set of cells, see Fig. 8. The equation system for the cell temperatures (including the actual hot gas temperature T_G) was solved with the target that the square sum of the heat flux balances of the cells reached a minimum.

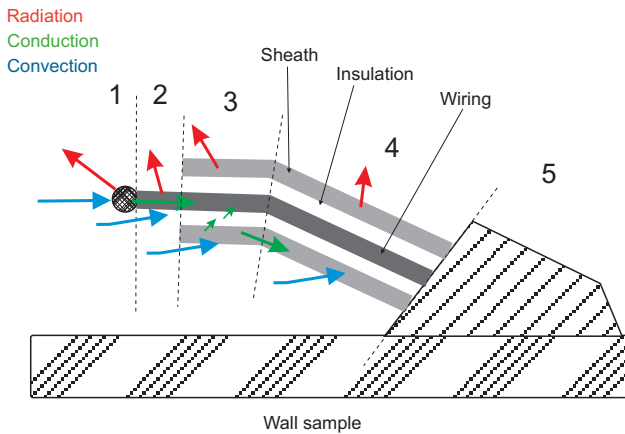


Fig. 8 Modelling of heat transfers in thermocouple

In Fig. 9 the corrected hot gas temperatures T_G for $T_F = 1750\text{K}$ and different pressures p and bulk gas velocities u are shown. The local hot gas temperature is fairly independent of the combustor pressure p and the bulk gas velocity u . In comparison to the homogeneous velocity distributions in Fig. 4...7 the temperature profiles reveal a different qualitative distribution. In the centre of the centre of the duct ($z = -15 \dots 15\text{mm}$) the measured gas temperature distribution is almost uniform. The overall temperature level is significantly ($\Delta T \approx 200\text{K}$) below the global flame temperature of the combustor $T_F = 1750\text{K}$. This difference can be attributed to the heat shield cooling air in the combustor, see section 3, cooling the exhaust gas at the outer circumference of the flow. In comparison to the wall boundary layer the mass flow is too large to be blown through the boundary layer bleed. At the moment the repeatability of the temperature measurements is not yet perfect. The overall level of the gas temperature is varying by $\Delta T \approx \pm 60\text{K}$, i. e. $\pm 4\%$ of the gas temperature T_G . These deviations are likely to be caused by minor changes of the fuel placement in the burner and inside the combustor. The error propagation leads to an uncertainty in the same order of magnitude ($\pm 4\%$) in the overall cooling effectiveness η calculated from the measured wall temperatures.

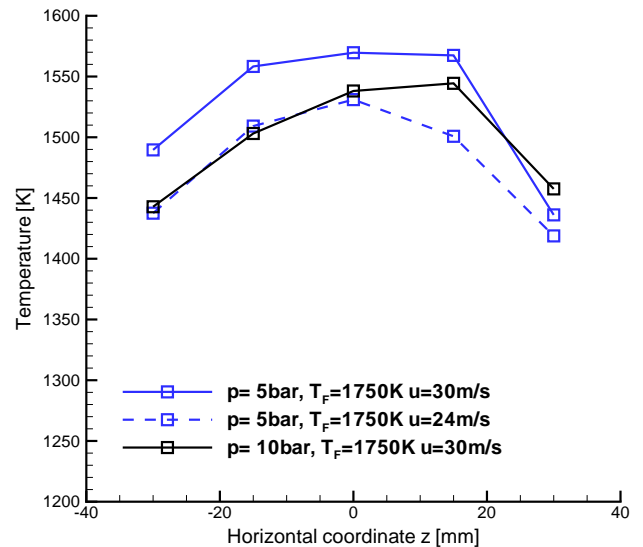


Fig. 9 Profiles of gas temperature T_G for different pressures p at $T_F = 1750\text{K}$, $y = 3\text{mm}$

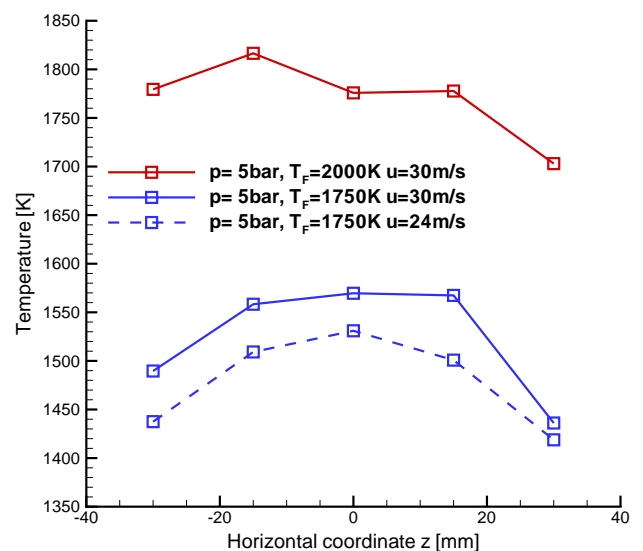


Fig. 10 Profiles of gas temperature T_G for different flame temperatures T_F at $p = 5\text{bar}$, $y = 3\text{mm}$

The influence of the global flame temperature T_F on the local gas temperature T_G is shown in Fig. 10. The difference in the global flame temperature T_F in the combustor can be found almost exactly in the local gas temperature T_G in the same qualitative distribution. The figures 6...10 indicate that the convective heat load on the test sample can be varied in the test section by set-

ting gas velocity, temperature and pressure almost independently at realistic gas turbine combustor conditions.

The effectiveness of the boundary layer bleed is shown in Fig. 11 for a global flame temperature $T_F = 2000\text{K}$ (TC3 in Table 1). When the boundary layer bleed is closed the local gas temperatures are $\Delta T = 50\dots 200\text{K}$ lower in comparison to the boundary layer bleed in operation. Furthermore the temperature distribution is much more uniform when the bleed is open.

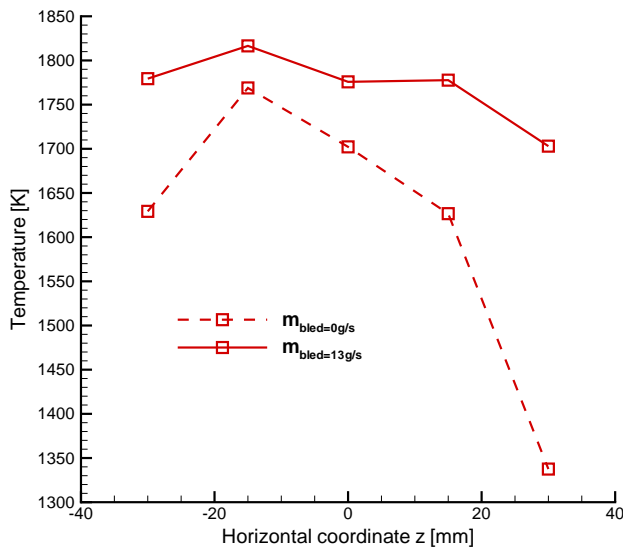


Fig. 11 Profiles of gas temperature T_G for different boundary layer bleed mass flows \dot{m}_{bleed} at $T_F = 2000\text{K}$, $y = 3\text{mm}$

6 Summary

In this contribution a new test rig for characterizing the cooling performance of gas turbine combustor wall elements was introduced. The target was to design a test rig which provides all typical gas turbine combustor flow characteristics like swirling flow field, temperature and velocity distribution and fluctuations. This was achieved by mounting the test section downstream of a combustor operated as a hot gas generator. A realistic and generic heat load is produced which is decoupled from the heat release distribution in the flame. By this means the analysis of the mea-

sured data and comparison with correlations and CFD results is made easier. Results of the flow characterisation upstream of the test sample were presented. The velocity distribution revealed the characteristics of a swirling combustor flow field. The gas temperature close to the wall was at a realistic level but showed larger inhomogeneities than the velocity distributions. The limited repeatability of the gas temperatures requires further investigations in order to reduce the present uncertainty of $\pm 4\%$ in the cooling effectiveness. Gas temperature, pressure and velocity can be set individually with only moderate effects on other flow properties allowing detailed investigations of the influence of the operating conditions on the cooling efficiency.

7 Acknowledgement

The authors gratefully acknowledge the helpful discussions and the support from Thomas Dörr and Miklós Gerendás at Rolls-Royce Deutschland. We also thank our colleagues in the department for combustor testing who were involved in the design, maintenance and operation of the test rig.

References

- [1] A. H. Lefebvre. The role of fuel preparation in low-emission combustion. *Journal of Engineering for Gas Turbines and Power*, 117:617 – 654, 1995.
- [2] V. J. Lyons. Fuel/air nonuniformity-effect on nitric oxide emissions. *AIAA-81-0327*, 1981.
- [3] W. J. Dodds and D. W. Bahr. Combustion system design. In A. M. Mellor, editor, *Design of modern gas turbine combustors*, chapter 4, pages 343 – 476. Academic Press, 1990.
- [4] S. Bake, M. Gerendás, W. Lazik, T. Dörr, and T. Schilling. Entwicklung eines Magerverbrennungskonzeptes zur Schadstoffreduzierung im Rahmen des nationalen Luftfahrtforschungsprogramms Engine 3E. In *Tagungsband der DGLR Jahrestagung, Paper 182*, 2004.
- [5] D. R. Ballal and A. H. Lefebvre. A proposed method for calculating film-cooled wall tem-

- peratures in gas turbine combustion chambers. *ASME 72-WA/HT-24*, 1972.
- [6] M. Martiny, A. Schulz, and S. Wittig. Full-coverage film cooling investigations: Adiabatic wall temperatures and flow visualization. *ASME 95-WA/HT-4*, 1995.
- [7] K. M. B. Gustafsson and T. G. Johansson. An experimental study of surface temperature distribution on effusion-cooled plates. *Journal of Engineering for Gas Turbines and Power*, 123:308 – 316, 2001.
- [8] D. Brauckmann and J. von Wolfersdorf. Infrared thermography with in-situ calibration using thermochromic liquid crystals applied to film cooling. *ASME GT2004-53855*, 2004.
- [9] M. D. Barringer, O. T. Richard, J. P. Walter, S. M. Stitzel, and K. A. Thole. Flow field simulations of a gas turbine combustor. *ASME 2001-GT-0170*, 2001.
- [10] S. W. Burd, R. W. Kaszeta, and T. W. Simon. Measurements in film cooling flows: Hole l/d and turbulence intensity effects. *Journal of Turbomachinery*, 120:791 – 798, 1998.
- [11] C. Saumweber, A. Schulz, and S. Wittig. Free-stream turbulence effects on film cooling with shaped holes. *ASME GT-2002-30170*, 2002.
- [12] J. E. Mayhew, J. W. Baugh, and A. R. Byerley. The effect of freestream turbulence on film cooling heat transfer coefficient and adiabatic effectiveness using compound angle holes. *ASME GT2004-53230*, 2004.
- [13] G. Meyers, J. Van der Geest, J. Sanborn, and F. Davis. Comparison of advanced cooling concepts using color thermography. *AIAA-85-1289*, 1985.
- [14] J. L. Champion and B. Deshaies. Experimental investigation of the wall flow and cooling of combustion chamber walls. *AIAA-95-2498*, 1995.
- [15] B. Leger, G. Schott, and G. Grienche. Experimental study of geometric effect for design of multihole cooling for combustion chamber walls. In *RTO-MP-069(I), AC/323(AVT-072/073)TP/47*, pages 10–1 – 10–9, 2003.
- [16] J. P. Feist and A. L. Heyes. Measurement of wall temperatures in gas turbine combustors using thermographic phosphors. *ISABE-2001-1140*, 2001.
- [17] D. Filsinger, S. Münz, A. Schulz, and S. Wittig. Experimental assessment of fiber-reinforced ceramics for combustor walls. *Journal of Engineering for Gas Turbines and Power*, 123:271 – 276, 2001.
- [18] M. Gerendás, K. Höschler, and T. Schilling. Development and modeling of angled effusion cooling for the BR715 low emission staged combustor core demonstrator. In *RTO-MP-069(I), AC/323(AVT-072/073)TP/47*, pages 11–1 – 11–12, 2003.
- [19] J. L. Champion, B. Deshaies, R. Curtelin, and M. Desauty. Aerodynamical structure of the wall flow over a wavy surface partially cooled by air injection through multiperforations. *AIAA-99-1016*, 1999.
- [20] S. Rouvreau, J. L. Champion, and B. Deshaies. Aerodynamic characterisations of the structure of the flow generated over a flat plate by air injection through multiperforations. In H. Z. Xiang and L. Xin, editors, *Proc. of 5th Aisa-Pacific International Symposium on Combustion and Energy Utilization*, pages 176 – 182, 1999.
- [21] H.-E. Albrecht, M. Borys, N. Damaschke, and C. Tropea. *Laser Doppler and Phase Doppler measurement techniques*. Springer Verlag, Berlin, 2003.
- [22] T. Behrendt, M. Carl, C. Fleing, M. Frodermann, J. Heinze, I. Röhle, C. Hassa, R. Lück-erath, U. Meier, Y. Schneider-Kühnle, D. Wolff-Gaßmann, C. Laible, and M. Ziegler. Experimentelle und numerische Untersuchung der Verbrennung im ebenen Sektor einer gestuften Brennkammer bei realistischen Betriebsbedingungen. In *Tagungsband der DGLR Jahrestagung, Paper 188*, 1999. ISSN 1438-1648.
- [23] W. Stricker, R. Lück-erath, U. Meier, and W. Meier. Temperature measurements in combustion – not only with CARS: a look back at one aspect of the European CARS workshop. *Journal of Raman Spectroscopy*, 34:922 – 931, 2003.